Reducing Heart Dose with Protons and Cardiac Substructure Sparing for Mediastinal Lymphoma Treatment

Kekoa Taparra, MD, PhD[1,2]*; Scott C. Lester, MD[1]; W. Scott Harmsen, MS[3]*; Molly Petersen[3]*; Ryan K. Funk, MD[1]; Miran J. Blanchard, MD[1]; Phillip Young, MD[4]; Joerg Herrmann, MD[5]; Ashley Hunzeker, CMD[1]; Heather Schultz, CMD, RTT[1]; Cynthia McCollough, PhD[1]; Alexandria Tasson, PhD[1]; Shuai Leng, PhD[4]; James A. Martenson, MD[1]; Thomas J. Whitaker, PhD[1]; Eric Williamson, MD[4]; Nadia N. Laack, MD[1]

[1]Department of Radiation Oncology, Mayo Clinic, Rochester, MN, USA
[2]Mayo Clinic Alix School of Medicine, Mayo Clinic, Rochester, MN, USA
[3]Division of Biomedical Statistics and Informatics, Mayo Clinic, Rochester, MN, USA
[4]Department of Diagnostic Radiology, Mayo Clinic, Rochester, MN, USA
[5]Department of Cardiology, Mayo Clinic, Rochester, MN, USA
*This author contributed to and was responsible for statistical analyses.

Abstract

Purpose: Electrocardiogram-gated computed tomography with coronary angiography can be used for cardiac substructure sparing (CSS) optimization, which identifies and improves avoidance of cardiac substructures when treating with intensity modulated radiotherapy (IMRT). We investigated whether intensity modulated proton therapy (IMPT) would further reduce dose to cardiac substructures for patients with mediastinal lymphoma.

Patients and Methods: Twenty-one patients with mediastinal lymphoma were enrolled and underwent electrocardiogram-gated computed tomography angiography during or shortly after simulation for radiotherapy planning. Thirteen patients with delineated cardiac substructures underwent comparative planning with both IMPT and IMRT. Plans were normalized for equivalent (95%) target volume coverage for treatment comparison.

Results: Thirteen patients met criteria for this study. The median size of the mediastinal lymphadenopathy was 7.9 cm at the greatest diameter. Compared with IMRT-CSS, IMPT-CSS significantly reduced mean dose to all cardiac substructures, including 3 coronary arteries and 4 cardiac valves. Use of IMPT significantly reduced average whole-heart dose from 9.6 to 4.9 Gy ($P < .0001$), and average mean lung dose was 9.7 vs 5.8 Gy ($P < .0001$). Prospectively defined clinically meaningful improvement was observed in at least 1 coronary artery in 9 patients (69%), at least 1 cardiac valve in 10 patients (77%), and whole heart in all 13 patients.

Conclusions: For patients with mediastinal lymphoma, IMPT-CSS treatment planning significantly reduced radiation dose to cardiac substructures. The significant improvements outlined in this study for proton therapy suggest possible clinical improvement in alignment with previous analyses of CSS optimization.

Keywords: cardiac substructure sparing; mediastinal lymphoma; protons; cardio-oncology; IMPT

Introduction

Early-stage lymphoma has >90% cure rates with chemoradiation therapy [1]. Radiation therapy (RT) serves as the single most effective modality for local disease control [2–4]. However, conventional RT has been associated with long-term cardiac toxicities and secondary malignancies [5–11]. Cardiac radiation is associated with a sixfold increased risk of heart failure, myocardial infarction, and valvular heart disease compared with nonirradiated survivors [10, 12–15]. Heart failure risk is RT dose dependent with significant risk occurring with >20 Gy dose to the heart [16]. This may explain observed oncologist biases toward RT omission in Hodgkin lymphoma (HL) treatment [17–19]. This is alarming considering that RT omission comes at the cost of reduced outcomes [2–4]. Therefore, advancements in RT delivery are imperative to reduce long-term cardiac valvular disease, morbidity, and mortality, while also maintaining survival outcomes.

Mean heart dose (MHD) and left ventricular dose have been traditionally used to study the relationship between mediastinal radiation and late cardiac disease effects [5, 20–22], with a linear increased risk of a major coronary event with MHD and relative risk increase of 7% per gray [22]. Recent data suggest that cardiac substructure dose predicts cardiovascular disease risk [23–25]. Risk of coronary artery stenosis was found to increase by 4.9% per gray to the coronary artery segment. These studies demonstrated a lack of correlation between mean coronary artery dose and MHD, suggesting that MHD is not an optimal surrogate for coronary artery dose exposure.

Conventional RT treatment planning includes computed tomography (CT) scanning for tumor localization [26]. However, dynamic movement through the cardiac and respiratory cycles presents challenges [27]. Recent work highlighted the feasibility and benefit of electrocardiogram (ECG)–gated CT angiography to generate an intensity-modulated radiotherapy (IMRT) with cardiac substructure sparing (CSS) optimization (IMRT-CSS) treatment plan [28, 29]. This technique resulted in modest reduction of dose to cardiac substructures compared with IMRT alone.

Use of IMRT may deposit x-rays into normal tissues, which may increase the risk of developing heart disease [10]. Intensity-modulated proton therapy (IMPT) offers superior targeting with normal tissue sparing [30, 31]. Pencil beam scanning proton therapy provides excellent coverage and local control while reducing dose to organs at risk (OARs) for patients with mediastinal HL [32]. Given the promising data with CSS optimization and the opening of our institution's proton therapy center in June 2015, we began to enroll patients that we intended to treat with IMPT. Our goal was to investigate the benefit of ECG-gated CT angiography with proton treatment planning. Here we outline our experiences comparing CSS optimization with both x-rays and protons for mediastinal lymphoma.

Materials and Methods

Patients Enrollment

Criteria for patient eligibility has been previously described [28]. Patients with biopsy proven mediastinal disease (HL or non-HL) were prospectively enrolled in an institutional review board–approved study. Exclusion criteria included pregnancy and/or severe renal insufficiency ,defined as a serum creatinine >1.9 mg/dL. Informed consent or assent was obtained from all patients or guardians. Clinical staging was based on Lugano modified Ann Arbor staging [33]. All patients underwent initial staging with fludeoxyglucose-18 positron emission tomography–CT. The decision to treat patients with proton versus x-rays was left to the discretion of the treating physician, but ultimately influenced by the patient's insurance coverage.

Simulation and Imaging Protocol

Details of patient simulation were outlined previously [28, 29, 34]. Briefly, all patients were imaged (Siemens Definition AS64, Siemens, Malvern, Pennsylvania) using a deep inspiration breath-hold (DIBH) and ECG-gated CT angiography in the treatment position. During simulation, 2 breath-hold scans were acquired with a slice thickness of 1.5 mm. A single slice was acquired 2 mm below the carina. This image was used to set a region of interest (ROI) in the ascending aorta. Next, 65 mL of iodinated contrast at 5 mL/s followed by 40 mL of saline at 5 mL/s was administered. After a 7-second scan delay, single images were acquired in 1-second intervals at the level of the ROI. The CT scanner monitors the average Hounsfield unit (HU) within the ROI and above 140 HU (a user-set threshold); the angiogram images were automatically acquired using a rotation time of 0.3 seconds. The Varian Real-time Position Management (RPM; Varian Medical Systems, Palo Alto, California) respiratory gating system and DIBH were used to immobilize the lungs and chest. While the cardiac data are initially broken up into 20 bins, only the best systolic and best diastolic phases are reconstructed based on automated Siemens software that

uses the phase that best aligns with the tail end of the T wave from the patient's ECG data. Thus, only the best systolic and diastolic phases were reconstructed at 1.5-mm slice thickness, which Siemens automatically selects. Immediately after the angiogram, while contrast is still circulating, a breath-hold image set was acquired. Immobilization was fabricated and customized during simulation.

Target and OAR Delineation

All contouring was completed on the standard, noncontrast CT scan from simulation. Target volumes were defined using standard involved-site radiotherapy principles [4, 35]. Standard OARs, including the heart as a singular structure, were also defined. Eight total cardiac substructures were captured—3 coronary arteries (left anterior descending [LAD], left circumflex [LCX], right coronary [RCA] arteries), 4 cardiac valves (aortic [AV], pulmonic [PV], mitral [MV], and tricuspid [TV] valves), and left ventricle (LV)—while whole heart and lungs were contoured separately. Each structure was contoured in systole and diastole, reviewed throughout the cardiac cycle, and combined to form a single OAR planning organ at risk volume (PRV) to account for cardiac motion. All subsequent structure dose reporting is in reference to the 4-dimensional OAR PRV.

Treatment Planning

Three plans (IMRT, IMRT-CSS, and IMPT-CSS) were generated using Eclipse planning software (Varian Inc, Palo Alto, California) [28, 29]. Our previous work compared IMRT with and without CSS optimization. In that report we confirmed the feasibility of this technique and found that CSS-optimized IMRT plans resulted in superior OAR sparing without compromising target coverage. As it was expected that, similar to our previous findings with IMRT, IMPT with CSS sparing would similarly result in superior OAR sparing without compromising target coverage, IMPT plans without CSS sparing were not generated. Briefly, the cardiac substructure sparing plans (IMRT-CSS and IMPT-CSS) used ECG-gated CT angiography images. The IMRT alone plans were optimized with the same target coverage normalization. Our primary treatment planning objectives were to (1) keep the mean dose per structure less than 15 Gy and (2) ensure that 100% of the prescription dose was covering at least 95% of the target volume. Secondary objectives were to keep maximum doses and least dose the hottest 0.03 cm^3 receives less than 15 Gy. Clinically meaningful improvement benchmarks were prospectively defined based on current literature that identified radiation dose ranges associated with increased cardiac valvular disease and coronary artery disease [10, 15, 16, 23–25]: percent of volume of coronary arteries receiving 15–25 Gy improvement >10% and/or percent of volume of coronary arteries receiving at least 30 Gy (V30Gy) improvement >5%; volume of cardiac valves receiving at least 20-30 Gy (V20-30) improvement of >10%; and MHD improvement ≥1 Gy. All plans were reviewed and ultimately selected solely at the discretion of the treating physician. The radiation treatment itself was not gated and occurred throughout the cardiac cycle.

Statistical Analyses

Statistical analysis was performed using GraphPad Prism v8.0 (GraphPad Software, Palo Alto, California). All dose parameters for each of the 10 structures of interest from IMRT-CSS and IMPT-CSS were compared by nonparametric 2-tailed paired t-test for statistical significance ($P <$ .05), with the alternative hypothesis being that there is a nonzero difference. Due to expected dose differences based on adenopathy site, each vessel was analyzed independently.

Results

Characteristics of Patients, Lymphomas, and Treatments

Patient, disease, and treatment characteristics are outlined in **Table 1**. Thirteen patients with biopsy-proven lymphoma and planned mediastinal RT who were prospectively enrolled in our imaging trial underwent retrospective comparison of IMRT-CSS and IMPT-CSS treatment planning. Patient age range at time of diagnosis was 14–53 years. Patient disease was staged between IIA and IVB and classified as HL (n = 11) or diffuse large B cell lymphoma (n = 2). Over two-thirds (69%) of the patients had ≥9 cm mediastinal adenopathy. Median prescription dose and fractionation were 30 Gy (range, 21–30 Gy) in 15 fractions (range, 14–15 fractions). All of the patients ultimately used the CSS optimization plan. The use of proton versus x-ray therapy was left to the discretion of the treating physician but was generally influenced by individual patient insurance coverage.

Table 1. Patient, lymphoma type, and treatment characteristics.

Characteristic	No. of patients (%) (n = 13)
Patient	
Median follow-up (range)	2.4 (0.4–3.9)
Age at diagnosis (y)	
<18	5 (38)
18–25	4 (31)
>18	4 (31)
Sex	
Female	6 (46)
Male	7 (54)
ECOG	
0	10 (77)
1	3 (23)
Primary disease	
Lymphoma type	
Hodgkin	11 (85)
Non-Hodgkin (DLBCL)	2 (15)
Ann Arbor Stage	
IIA	4 (31)
IIB	6 (46)
IVA	1 (8)
IVB	2 (15)
Staging tests	
PET/CT	13 (100)
Bone marrow biopsy	12 (92)
Mediastinal mass	
<5 cm	2 (15)
5–10 cm	5 (38)
>10	6 (46)
No. of sites	
2	2 (15)
3	3 (23)
4 or more	8 (62)
Extranodal disease sites	
0	10 (77)
1	1 (8)
2	2 (15)
Prognosis	
Favorable	3 (23)
Unfavorable	3 (23)
Advanced	7 (54)
Treatment	
Initial therapy	
ABVD (2–4 cycles)	4 (31)
ABVD (6 cycles)	4 (31)
ABVE-PC (4 cycles)	2 (15)
BEACOPP	2 (15)
R-CHOP	1 (8)
Deauville	
1	6 (46)
2	4 (31)
3	1 (8)
Not scored	2 (15)

Table 1. Continued.

Characteristic	No. of patients (%) (n = 13)
Radiation modality	
IMRT	4 (31)
IMPT	9 (69)
Deep inspiratory breath hold	
Completed	11 (84)
Unable to complete	1 (8)
Missing information	1 (8)
Dose and fractionation	
Median (Gy)/fractions	30/15
Range (Gy)	21–30
Plan used for treatment	
Cardiac substructure sparing	13 (100)

Abbreviations: ABVD, adriamycin, bleomycin, vinblastine, and dacarbazine; ABVE-PC, doxorubicin, bleomycin, vincristine, etoposide, prednisone, and cyclophosphamide. BEACOPP, bleomycin, etoposide, doxorubicin, cyclophosphamide, vincristine, procarbazine, prednisone; DLBCL, diffuse large B-cell lymphoma; ECOG, Eastern Cooperative Oncology Group; PET/CT, positron emission tomography/computed tomography; IMPT, intensity modulated proton therapy; IMRT, intensity modulated radiation therapy; R-CHOP, rituximab, cyclophosphamide, doxorubicin, vincristine, prednisone.

General Doses Delivered for Treatments

Representative images of color-wash dose distributions for each of the 3 treatment plans (IMRT, IMRT-CSS, and IMPT-CSS) are displayed in **Figure 1**. Both coronary arteries and cardiac valves revealed trends toward sparing radiation dose with the use of IMPT treatment planning with CSS optimization. Threshold was set at a minimum of 15 Gy and a maximum of 32 Gy (shown on colorimetric scale). **Figure 2** summarizes the average radiation dose to volume histograms (DVHs) for each of the 10 structures of interest. **Tables 2, 3,** and **4** show the specific DVH parameters assessed for standard OAR, coronary arteries, and cardiac valves, respectively.

IMRT-CSS Versus IMPT-CSS Radiation Exposure to Standard OARs

Table 2 and **Supplemental Figure S1** show the comparison of DVH parameters for the whole heart, LV, and total lung between IMRT-CSS and IMPT-CSS treatment plans. Nearly all whole-heart and LV DVH parameters assessed showed an improvement with IMPT-CSS. Overall, the mean dose to the whole heart, LV, and total lung was significantly lower with IMPT for all DVH parameters assessed. IMPT-CSS reduced MHD (median, 4.9 vs 9.6 Gy), mean LV dose (median, 1.1 vs 6.6 Gy), and mean total lung dose (median, 5.8 vs 9.7 Gy) compared with IMRT-CSS. The IMPT-CSS treatment plan had a significantly improved volume of whole heart receiving at least 15 Gy, 20 Gy, and 25 Gy (V15Gy, V20Gy, and V25Gy). Similarly, the MPT-CSS treatment plan showed significantly improved volume of LV receiving at least 15 and 20 Gy (V15Gy and V20Gy) compared with IMRT-CSS. Clinically meaningful improvement with use of IMPT-CSS for MHD was achieved in 100% of patients, shown in **Supplemental Figure S2.**

Figure 1. IMRT, IMRT-CSS, and IMPT-CSS treatment plans for patients with HL. IMPT-CSS treatment planning reduces volume of cardiac substructures receiving 15 Gy (V15Gy) exposure to both coronary arteries (eg, left anterior descending artery) and cardiac valves (eg, aortic valve) compared with IMRT-CSS treatment planning in representative patients with HL. Color-wash dose distribution scale shows doses 15–32 Gy. All structures are PRVs based on 4-dimensional ECT-gated CT cardiac anatomy to account for motion of the structures. Abbreviations: CSS, cardiac substructure sparing; CT, computed tomography; ECG, electrocardiogram; HL, Hodgkin lymphoma; IMPT, intensity-modulated proton therapy; IMRT, intensity-modulated radiation therapy; PRV, planning organ at risk volume.
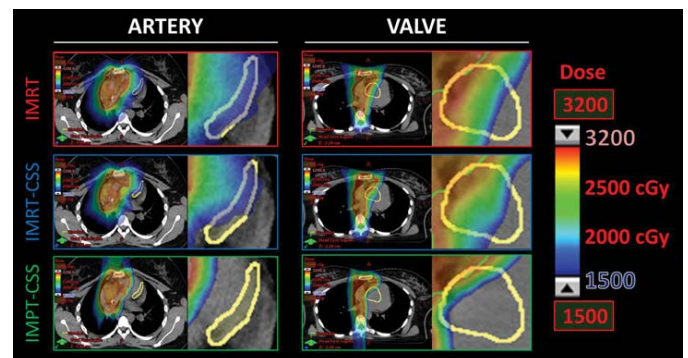
Figure 2. Mean DVHs for 10 structures for 3 types of treatment plans. Overall DVH curves for percent structure volume per given dose 0–30 Gy (V0-30Gy) of IMRT, IMRT-CSS, and IMPT-CSS. All structures are PRVs based on 4-dimrnsional ECT-gated CT cardiac anatomy to account for motion of the structures. Abbreviations: CSS, cardiac substructure sparing; CT, computed tomography; DVH, dose-volume histogram; ECG, electrocardiogram; IMPT, intensity-modulated proton therapy; IMRT, intensity-modulated radiation therapy; PRV, planning organ at risk volume.
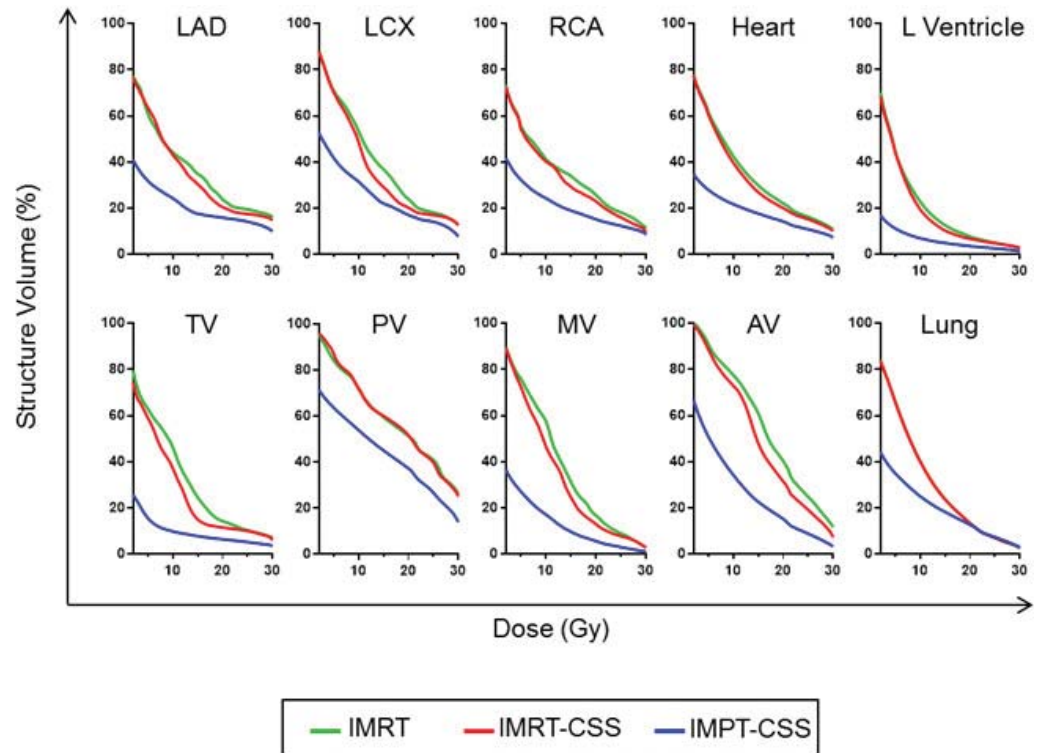
IMRT-CSS Versus IMPT-CSS Radiation Exposure to Coronary Arteries

Table 3 and **Supplemental Figure S3** show the comparison of radiation exposure to 3 coronary arteries (LAD, LCX, and RCA) between IMRT-CSS versus IMPT-CSS treatment plans. Overall, the mean dose to all 3 coronary arteries was significantly lower with IMPT for all DVH parameters assessed. Compared with IMRT-CSS, IMPT-CSS had an average mean dose improvement for LAD, LCX, and RCA of 4.7 Gy, 4.0 Gy, and 4.0 Gy, respectively. The average improvement with IMPT-CSS for LAD, LCX, and RCA receiving at least 15 Gy (V15Gy) was 12.8%, 7.0%, and 10.3%, respectively. The number of patients who achieved clinically meaningful improvement for LAD, LCX, and RCA were 6 (46%), 5 (38%), and 6 (46%), respectively, as shown in **Supplemental Figure S2**. Nine patients (69%) had >10% improvement in at least 1 coronary artery for the V15-30Gy DVH parameters. Four patients had an LAD V15Gy improvement with IMPT-CSS >10% (range, 10.7%–66.0%). Only t2 patients showed an increased dose of more than 1% to a single coronary artery with IMPT-CSS relative to IMRT-CSS (2.9% to the LCX and 1.2% to the LAD).

IMRT-CSS Versus IMPT-CSS Radiation Exposure to Cardiac Valves

Table 4 and **Supplemental Figure S4** show the comparison of radiation exposure to the 4 cardiac valves (TV, PV, MV, and AV) using IMRT-CSS versus IMPT-CSS treatment plans. Overall, the mean dose to all 4 cardiac valves was significantly lower with IMPT for all DVH parameters assessed. The average mean dose improvement of IMPT-CSS compared with IMRT-CSS for AV, MV, PV, and TV were 7.3 Gy, 6.6 Gy, 5.2 Gy, and 5.8 Gy, respectively. The average improvement with IMPT-CSS over IMRT-CSS for the volume of AV, MV, PV, and TV receiving at least 20 Gy (V20Gy) was 16.3%, 7.4%, 14.5%, and 15.1%, respectively. The number of patients who achieved clinically meaningful improvement for AV, MV, PV, and TV were 9 (69%), 6 (46%), 9 (69%), and 3 (23%), respectively as shown in **Supplemental Figure S2**. Aortic and pulmonary valves had significant improvement with IMPT-CSS at the V20Gy and V25Gy DVH parameters. Ten patients (77%) had >10% of V20Gy with IMPT-CSS in at least 1 valve, half of which had >10% improvements in 3 of 4 valves. One patient did have an increase in the aortic valve V30Gy by 10.6% with IMPT, and no significant benefit for the other valves with IMPT.

Discussion

The present study demonstrates the utility of combining our ECG-gated CT angiography derived CSS optimization with proton therapy (IMPT-CSS) to reduce dose to heart and cardiac substructures. Our CSS optimization addresses the challenge of

Table 2. Radiation dose of thoracic contents with IMRT-CSS versus IMPT-CSS.

Structure PRV, parameter	IMRT-CSS Median (IQR)	SD	IMPT-CSS Median (IQR)	SD	Median difference	Mean difference	Paired t-test (P)
Heart							
Mean (Gy)	9.6 (6.4–16.3)	5.5	4.9 (2.4–8.9)	3.9	−5.1	−4.8	<.0001
Maximum (Gy)	32.7 (26.0–33.0)	4.8	32.6 (29.4–33.5)	4.1	0.3	1.1	.1492
V_{5Gy} (%)	73.4 (32.6–85.1)	29.6	25.3 (13.6–40.9)	14.9	−32.2	−32.6	.0002
V_{10Gy} (%)	36.4 (19.9–61.3)	21.5	19.7 (9.4–33.4)	13.9	−18.3	−17.9	.0002
V_{15Gy} (%)	20.4 (10.8–44.3)	19.0	14.3 (6.7–28.0)	13.3	−10.0	−9.2	.0007
V_{20Gy} (%)	12.6 (4.8–36.2)	17.7	10.3 (3.2–23.2)	12.7	−2.5	−5.8	.0108
V_{25Gy} (%)	9.9 (0.1–29.4)	16.5	7.3 (0.3–18.8)	12.0	−1.2	−4.4	.0431
V_{30Gy} (%)	5.3 (0.0–20.6)	13.1	4.0 (0.0–12.5)	9.6	−0.0	−2.8	.2024
Left ventricle							
Mean (Gy)	6.6 (2.4–10.2)	4.6	1.1 (0.1–3.7)	2.7	−5.6	−4.4	<.0001
Maximum (Gy)	22.0 (10.4.0–31.7)	10.7	18.9 (10.9–28.1)	10.9	−0.1	−2.4	.0851
V_{5Gy} (%)	53.2 (7.6–78.0)	36.0	7.8 (0.3–22.0)	12.8	−34.3	−33.0	.0022
V_{10Gy} (%)	15.1 (0.2–34.4)	18.0	1.5 (0.0–12.9)	10.2	−15.1	−12.5	.0013
V_{15Gy} (%)	4.2 (0.0–17.6)	14.5	0.2 (0.0–8.5)	8.5	−3.7	−5.4	.0098
V_{20Gy} (%)	0.1 (0.0–11.2)	11.9	0.0 (0.0–5.7)	6.9	0.0	−3.1	.0468
V_{25Gy} (%)	0.0 (0.0–7.8)	9.1	0.0 (0.0–3.4)	5.3	0.0	−2.2	.0611
V_{30Gy} (%)	0.0 (0.0–4.6)	5.6	0.0 (0.0–1.1)	3.2	0.0	−1.4	.0795
Lung							
Mean (Gy)	9.7 (7.6–11.8)	2.6	5.8 (4.6–6.7)	2.5	−3.4	−3.6	.0001
Maximum (Gy)	32.7 (26.0–33.0)	4.3	33.0 (30.1–33.6)	3.9	0.5	1.2	.0942
V_{5Gy} (%)	65.2 (51.7–77.4)	15.3	36.0 (25.2–42.2)	10.9	−26.4	−30.9	<.0001
V_{10Gy} (%)	41.1 (29.5–50.2)	12.2	24.0 (18.6–27.4)	9.2	−12.7	−15.1	.0003
V_{15Gy} (%)	25.2 (15.8–28.1)	9.6	16.8 (12.3–18.9)	8.6	−2.1	−5.4	.0896
V_{20Gy} (%)	12.2 (6.3–18.5)	8.1	10.9 (7.2–13.3)	8.4	0.0	−0.6	.7992
V_{25Gy} (%)	8.7 (0.3–12.0)	5.9	6.4 (1.3–9.2)	7.7	0.0	0.4	.8353
V_{30Gy} (%)	3.2 (0.0–5.1)	2.8	1.9 (0.0–3.7)	4.0	0.0	0.0	.9842

Abbreviations: CSS, cardiac substructure sparing; IMPT, intensity modulated proton therapy; IMRT, intensity modulated radiation therapy; IQR, interquartile range; PRV, planning organ at risk volume; SD, standard deviation; V_{xGy}, volume of coronary arteries receiving at least X Gy.

accounting for dynamic cardiac and respiratory cycle motion. Use of IMPT-CSS provides further dosimetric benefit across the entire dose-volume histogram, as depicted in **Figure 1**. Our IMRT-CSS treatment plan provided slight benefit compared with standard IMRT, particularly for V15Gy-V20Gy.

In this study, we focused on the higher dose range DVH parameters (V15Gy-V30Gy) due to the conventional understanding of cardiac toxicity and radiation dose [7, 10, 15, 36]. Doses >20 Gy to the heart have been associated with an increased risk of heart failure [16]. Among the majority of structures analyzed, the average reduction at the V15Gy with IMPT-CSS compared with IMRT-CSS was significant but modest. However, even small dosimetric improvements are clinically relevant: a recent predictive model for ischemic cardiac events highlighted LAD V5Gy, LCX V20Gy, and age as a model that outcompeted more traditional models using whole-heart dose and age [37]. Further work suggested that MHD is not a proper surrogate for predicting cardiac toxicity compared with coronary arteries [23].

In our study, average MHD was reduced from 9.6 to 4.9 Gy using IMRT-CSS and IMPT-CSS, respectively. Cardiac substructure dose was generally reduced with CSS optimization. The LAD showed a median V5Gy of 62.9% and 20.5% for IMRT-CSS and IMPT-CSS, respectively. Given steep dose gradients across the heart with protons, CSS optimization may reduce high doses to cardiac substructures that may not be accounted for by the MHD parameter alone. Thus, even seemingly small improvements in RT dose may potentially have a greater impact on reducing cardiac risk than previously appreciated.

Regarding dosimetric improvement to cardiac valves, our IMPT-CSS treatment plan outperformed the IMRT-CSS treatment plan for nearly every dosimetric parameter, including mean structure PRV dose. Aortic and mitral valves are most commonly reported to have involvement with long-term cardiac valvular disease [36]. Significant improvements were reported for mitral

Table 3. Radiation dose to coronary arteries with IMRT-CSS versus IMPT-CSS.

Structure PRV, parameter	IMRT-CSS Median (IQR)	SD	IMPT-CSS Median (IQR)	SD	Median difference	Mean difference	Paired t-test (P)
LAD							
Mean (Gy)	9.6 (7.0–16.8)	7.6	2.7 (1.8–11.6)	8.3	–3.7	–4.7	.0003
Maximum (Gy)	22.2 (14.2–31.3)	9.3	15.8 (12.5–31.6)	11.0	–1.0	–2.4	.031
V_{5Gy} (%)	62.9 (52.4–90.2)	32.2	20.5 (11.7–50.7)	28.4	–21.5	–31.8	.0046
V_{10Gy} (%)	43.2 (20.1–57.1)	31.0	10.0 (2.6–44.0)	29.1	–9.3	–18.8	.0245
V_{15Gy} (%)	31.5 (0.0–53.1)	31.7	0.6 (0.0–38.3)	29.3	0.0	–12.8	.0505
V_{20Gy} (%)	4.8 (0.0–44.7)	29.6	0.0 (0.0–33.1)	28.1	–0.4	–4.6	.0176
V_{25Gy} (%)	0.0 (0.0–40.5)	29.6	0.0 (0.0–26.1)	26.4	0.0	–3.3	.0563
V_{30Gy} (%)	0.0 (0.0–29.9)	26.4	0.0 (0.0–6.2)	23.8	0.0	–4.8	.0788
LCX							
Mean (Gy)	11.0 (6.4–15.30)	8.2	5.8 (1.8–11.1)	8.8	–3.3	–4.0	<.0001
Maximum (Gy)	22.1 (17.2–31.3)	8.7	22.1 (12.6–31.2)	10.3	–0.6	–2.4	.0505
V_{5Gy} (%)	68.9 (51.8–100.0)	31.8	40.2 (12.2–64.5)	32.8	–17.8	–28.4	.004
V_{10Gy} (%)	51.8 (11.4–81.3)	34.6	20.7 (2.9–54.5)	32.4	–9.4	–17.2	.0282
V_{15Gy} (%)	14.8 (2.2–46.0)	32.7	6.6 (0.0–39.6)	32.3	–0.1	–7.0	.0853
V_{20Gy} (%)	2.9 (0.0–30.4)	32.7	2.3 (0.0–23.0)	31.7	–0.2	–3.1	.0842
V_{25Gy} (%)	0.0 (0.0–25.3)	32.3	0.0 (0.0–14.5)	30.2	–0.0	–2.9	.0614
V_{30Gy} (%)	0.0 (0.0–16.0)	27.6	0.0 (0.0–9.8)	16.2	–0.0	–4.8	.2047
RCA							
Mean (Gy)	11.5 (2.5–14.6)	8.4	3.4 (0.5–9.4)	8.0	–3.5	–4.0	.001
Maximum (Gy)	21.6 (13.2–31.7)	10.2	19.4 (8.6–31.6)	11.6	–1.0	–2.3	.0401
V_{5Gy} (%)	57.8 (13.3–92.8)	37.8	24.8 (2.6–55.4)	32.0	–15.8	–22.1	.0089
V_{10Gy} (%)	30.3 (6.9–77.1)	35.6	7.4 (0.4–36.3)	31.6	–6.2	–15.9	.0253
V_{15Gy} (%)	28.4 (0.0–46.4)	34.3	0.7 (0.0–29.3)	30.3	–3.5	–10.3	.0458
V_{20Gy} (%)	2.3 (0.0–35.4)	31.7	0.0 (0.0–23.5)	25.0	–1.9	–7.8	.0477
V_{25Gy} (%)	0.0 (0.0–24.3)	23.9	0.0 (0.0–18.2)	22.0	0.0	–3.6	.0691
V_{30Gy} (%)	0.0 (0.0–13.4)	17.8	0.0 (0.0–8.8)	18.3	0.0	–0.9	.2553

Abbreviations: CSS, cardiac substructure sparing; IMPT, intensity modulated proton therapy; IMRT, intensity modulated radiation therapy; IQR, interquartile range; LAD, left anterior descending artery; LCX, left circumflex artery; PRV, planning organ at risk volume; RCA, right coronary artery; SD, standard deviation; V_{xGy}, volume of coronary arteries receiving at least X Gy.

and tricuspid valves, but not aortic or pulmonic valves [38]. In our study, mean radiation doses to all 4 valves were significantly reduced with IMPT-CSS.

Our findings are particularly relevant given a recent report outlining changing attitudes regarding RT in the setting of HL treatment over the past 2 decades [17]. A large analysis using the National Cancer Institute's Surveillance, Epidemiology, and End Results (SEER) database found an increase in RT omission for patients with HL over the most recent decades. Omission of RT was independently associated with increased patient mortality among adolescents and young adults with HL without any reduction of secondary malignancies. Omission of RT was due in part to cardiotoxicity. Therefore, our work, if confirmed by others, has the possibility to decrease concerns regarding RT's role in HL therapy by addressing cardiac toxicity outcomes of HL survivors.

Limitations of this study include lack of comparison with IMPT performed without CSS sparing. Based on our prior work both clinically (patients treated clinically who were not enrolled on the protocol) as well as our prior work comparing CSS-sparing with IMRT, we felt it exceedingly unlikely that IMPT without intentional CSS-sparing would show similar or improved OAR sparing, but there may be cases in which target volume is minimally proximal to OARs, and CSS-sparing provides little additional benefit. In addition, although treatment was delivered with respiratory motion management, treatment was not cardiac-gated. The PRVs for all CSSs were generated based on the 4D ECT-gated treatment planning CT to account for cardiac motion, which resulted in a larger OAR avoidance area than if treatment were possible with cardiac gating. Despite the large PRVs, CSS-IMPT still resulted in meaningful reductions in OAR PRV dose without compromising coverage for most

Table 4. Radiation dose to cardiac valves with IMRT-CSS versus IMPT-CSS.

Structure PRV, parameter	IMRT-CSS [%] Median (IQR)	SD	IMPT-CSS [%] Median (IQR)	SD	Median difference	Mean difference	Paired t-test (P)
AV							
Mean (Gy)	17.1 (8.6–22.0)	7.0	7.4 (3.7–14.9)	5.7	−6.2	−7.3	<.0001
Maximum (Gy)	29.0 (19.7–31.0)	6.1	28.2 (17.5–31.9)	8.4	−0.4	−1.8	.2041
V_{5Gy} (%)	100.0 (76.0–100.0)	19.5	49.7 (25.8–78.0)	29.6	−34.8	−37.7	<.0001
V_{10Gy} (%)	95.6 (31.5–99.7)	36.9	30.5 (10.6–60.8)	26.0	−34.1	−38.7	.0001
V_{15Gy} (%)	61.5 (9.1–81.2)	36.9	14.9 (1.8–46.3)	22.9	−24.7	−25.4	.0006
V_{20Gy} (%)	33.0 (1.6–60.5)	31.3	7.6 (0.0–36.4)	17.5	−10.9	−16.3	.0055
V_{25Gy} (%)	1.9 (0.0–40.2)	25.4	0.7 (0.0–25.0)	12.4	−1.9	−10.3	.025
V_{30Gy} (%)	0.0 (0.0–10.4)	14.1	0.0 (0.0–6.9)	5.4	−0.0	−4.0	.2157
MV							
Mean (Gy)	9.2 (7.3–15.2)	5.5	3.7 (0.7–7.2)	3.8	−4.8	−6.6	<.0001
Maximum (Gy)	23.5 (14.3–31.0)	8.9	22.2 (9.7–31.0)	11.7	−0.6	−3.0	.0431
V_{5Gy} (%)	85.7 (50.1–100.0)	34.3	25.4 (3.6–41.0)	25.6	−34.9	−45.4	.0003
V_{10Gy} (%)	38.9 (17.7–83.7)	35.0	14.3 (0.1–29.5)	19.1	−20.4	−29.6	.0034
V_{15Gy} (%)	19.2 (4.0–44.4)	23.1	7.2 (0.0–15.6)	11.4	−8.5	−14.9	.0071
V_{20Gy} (%)	4.9 (0.0–18.7)	18.9	1.9 (0.0–7.5)	8.9	−0.8	−7.4	.0559
V_{25Gy} (%)	0.0 (0.0–5.5)	16.3	0.0 (0.0–3.6)	6.2	0.0	−4.7	.1637
V_{30Gy} (%)	0.0 (0.0–0.5)	7.8	0.0 (0.0–0.5)	3.3	0.0	−1.7	.1988
PV							
Mean (Gy)	18.5 (9.8–28.3)	8.4	12.7 (6.5–22.2)	8.8	−4.9	−5.2	.0001
Maximum (Gy)	31.5 (22.9–32.5)	5.9	31.8 (26.6–32.6)	4.9	0.4	1.4	.1171
V_{5Gy} (%)	100.0 (77.1–100.0)	18.9	65.3 (31.8–98.7)	31.7	−20.3	−23.6	.0063
V_{10Gy} (%)	72.5 (42.8–100.0)	29.6	47.6 (24.7–93.1)	33.6	−15.0	−18.2	.0031
V_{15Gy} (%)	59.0 (25.8–100.0)	35.8	39.2 (15.1–83.7)	33.4	−13.7	−15.0	.0042
V_{20Gy} (%)	50.8 (12.8–93.6)	37.5	31.6 (10.4–67.7)	30.9	−10.9	−14.5	.0096
V_{25Gy} (%)	44.9 (0.0–76.6)	36.1	17.5 (3.0–45.6)	28.2	−11.6	−13.1	.0198
V_{30Gy} (%)	6.5 (0.0–52.9)	29.1	3.9 (0.0–21.2)	21.1	0.0	−11.1	.0511
TV							
Mean (Gy)	7.1 (2.6–12.8)	8.1	0.3 (0.0–5.2)	5.8	−4.9	−5.8	<.0001
Maximum (Gy)	14.8 (7.4–21.9)	9.8	4.4 (1.1–19.4)	12.4	−6.4	−5.6	.0036
V_{5Gy} (%)	70.5 (10.8–100.0)	44.0	0.0 (0.0–37.3)	25.9	−51.5	−43.4	.0008
V_{10Gy} (%)	23.8 (0.4–81.0)	41.2	0.0 (0.0–12.5)	21.4	−4.3	−27.3	.0166
V_{15Gy} (%)	0.0 (0.0–16.1)	30.2	0.0 (0.0–5.8)	18.7	0.0	−7.1	.0667
V_{20Gy} (%)	0.0 (0.0–3.1)	29.2	0.0 (0.0–2.4)	16.5	0.0	−5.1	.1751
V_{25Gy} (%)	0.0 (0.0–0.2)	26.9	0.0 (0.0–0.6)	14.3	0.0	−4.8	.1999
V_{30Gy} (%)	0.0 (0.0–0.0)	15.3	0.0 (0.0–0.0)	10.9	0.0	−2.4	.1838

Abbreviations: AV, aortic valve; CSS, cardiac substructure sparing; IMPT, intensity modulated proton therapy; IMRT, intensity modulated radiation therapy; IQR, interquartile range; LV, left ventricle; MV, mitral valve; PRV, planning organ at risk volume; PV, pulmone valve; SD, standard deviation; TV, tricuspid valve; V_{xGy}, volume of coronary arteries receiving at least X Gy.

patients. Although further reductions in CSS dose may be possible with cardiac-gated treatment, current technology limitations of prolonged beam time and patient fatigue during multiple breath-holds may make further gating impractical for most patients.

Additional limitations include the small sample size and the lack of long-term cardiac health data. The wide anatomic variation of the heart and coronary vessels may not be accounted for in this current study given the sample size. Despite this, our patients underwent weekly verification scans to allow for adaptive radiotherapy during each patient's treatment to compensate for any anatomic or tumor evolution on treatment. Furthermore, validation on an external cohort will be necessary before definitive conclusions can be drawn regarding the efficacy of IMPT in reducing cardiac toxicity. Follow-up in larger patient cohorts will be necessary to evaluate the actual clinical impact on long-term coronary artery disease, valvular heart disease, and overall cardiac morbidity.

It is possible that this methodology may be applied to other malignancies involving the mediastinal structures abutting the heart. Proton therapy provides a potential advantage over IMRT by delivering conformal, high-dose radiation to the target with high precision of normal tissue sparing. A reported small dose reduction in the setting of breast cancer with IMRT and DIBH recently demonstrated a meaningful benefit to cardiac health as measured by cardiac left ventricular ejection fraction [39]. Similar dosimetric improvements to the heart were recently described in lung cancer patients treated with proton therapy [40]. Our study would suggest that the combination of CSS optimization with proton therapy might further enhance the improvements seen in the setting of breast and lung cancer.

Overall, our study demonstrated that RT planning using ECG-gated CT angiography is feasible. In our small cohort, there was meaningful dose reduction to critical cardiac structures without increasing overall heart and lung mean dose compared with conventional planning. In combination with protons, our data suggest that IMPT-CSS achieved superior and potentially clinically meaningful coronary sparing compared with IMRT-CSS and IMRT alone. The implications of these findings suggest that the use of protons and CSS optimization for future patients with HL and other mediastinal malignancies may reduce long-term cardiac dysfunction through reduced radiation dose exposure to coronary arteries and cardiac valves.

Conclusion

The present study has illuminated potential clinical benefits and dosimetric advantages of combining advanced cardiac substructure sparing (CSS) optimization with proton radiotherapy.

ADDITIONAL INFORMATION AND DECLARATIONS

References

1. Smith MA, Seibel NL, Altekruse SF, Ries LAG, Melbert DL, O'Leary M, Smith FO, Reaman GH. Outcomes for children and adolescents with cancer: challenges for the twenty-first century. *J. Clin. Oncol.* 2010;28:2625–2634.

2. Raemaekers JMM, André MPE, Federico M, Girinsky T, Oumedaly R, Brusamolino E, Brice P, Fermé C, van der Maazen R, Gotti M, Bouabdallah R, Sebban CJ, Lievens Y, Re A, Stamatoullas A, Morschhauser F, Lugtenburg PJ, Abruzzese E, Olivier P, Casasnovas R-O, van Imhoff G, Raveloarivahy T, Bellei M, van der Borght T, Bardet S, Versari A, Hutchings M, Meignan M, Fortpied C. Omitting radiotherapy in early positron emission tomography-negative stage I/II Hodgkin lymphoma is associated with an increased risk of early relapse: Clinical results of the preplanned interim analysis of the randomized EORTC/LYSA/FIL H10 trial. *J. Clin. Oncol.* 2014;32:1188–1194.

3. Radford J, Illidge T, Counsell N, Hancock B, Pettengell R, Johnson P, Wimperis J, Culligan D, Popova B, Smith P, McMillan A, Brownell A, Kruger A, Lister A, Hoskin P, O'Doherty M, Barrington S. Results of a trial of PET-directed therapy for early-stage Hodgkin's lymphoma. *N. Engl. J. Med.* 2015;372:1598–1607.

4. Specht L, Yahalom J, Illidge T, Berthelsen AK, Constine LS, Eich HT, Girinsky T, Hoppe RT, Mauch P, Mikhaeel NG, Ng A. Modern radiation therapy for Hodgkin lymphoma: Field and dose guidelines from the international lymphoma radiation oncology group (ILROG). *Int. J. Radiat. Oncol. Biol. Phys.* 2014.

5. Tukenova M, Guibout C. Role of Cancer Treatment in Long-Term Overall and Cardiovascular Mortality After Childhood Cancer. *J. Clin. Oncol.* 2010;28:1308–1316.

6. Daniels LA, Krol ADG, De Graaf MA, Scholte AJHA, Van't Veer MB, Putter H, de Roos A, Schalij MJ, Creutzberg CL. Screening for coronary artery disease after mediastinal irradiation in Hodgkin lymphoma survivors: Phase II study of indication and acceptance. *Ann. Oncol.* 2014;25:1198–1203.

7. van der Pal HJ, van Dalen EC, van Delden E, van Dijk IW, Kok WE, Geskus RB, Sieswerda E, Oldenburger F, Koning CC, van Leeuwen FE, Caron HN, Kremer LC. High risk of symptomatic cardiac events in childhood cancer survivors. *J. Clin. Oncol.* 2012;30:1429–1437.

8. Carvalho S, Catarino TA, Dias AM, Kato M, Almeida A, Hessling B, Figueiredo J, Gartner F, Sanches JM, Ruppert T, Miyoshi E, Pierce M, Carneiro F, Kolarich D, Seruca R, Yamaguchi Y, Taniguchi N, Reis CA, Pinho SS. Preventing E-cadherin aberrant N-glycosylation at Asn-554 improves its critical function in gastric cancer. *Oncogene*. 2015:1–13.

9. Galper SL, Yu JB, Mauch PM, Strasser JF, Silver B, Lacasce A, Marcus KJ, Stevenson MA, Chen MH, Ng AK. Clinically significant cardiac disease in patients with Hodgkin lymphoma treated with mediastinal irradiation. *Blood*. 2011;117:412–418.

10. Van Nimwegen FA, Schaapveld M, Janus CPM, Krol ADG, Petersen EJ, Raemaekers JMM, Kok WEM, Aleman BMP, Van Leeuwen FE. Cardiovascular disease after hodgkin lymphoma treatment 40-year disease risk. *JAMA Intern. Med*. 2015.

11. Bhatia S, Yasui Y, Robison LL, Birch JM, Bogue MK, Diller L, DeLaat C, Fossati-Bellani F, Morgan E, Oberlin O, Reaman G, Ruymann FB, Tersak J, Meadows AT. High Risk of Subsequent Neoplasms Continues With Extended Follow-Up of Childhood Hodgkin's Disease: Report From the Late Effects Study Group. *J. Clin. Oncol*. 2003;21:4386–4394.

12. Burstein HJ. Cognitive side-effects of adjuvant treatments. *Breast*. 2007;16 Suppl 2:S166–8.

13. Stewart JR, Fajardo LF, Gillette SM, Constine LS. Radiation injury to the heart. *Int. J. Radiat. Oncol. Biol. Phys*. 1995;31:1205–1211.

14. Mulrooney DA, Yeazel MW, Kawashima T, Mertens AC, Mitby P, Stovall M, Donaldson SS, Green DM, Sklar CA, Robison LL, Leisenring WM. Cardiac outcomes in a cohort of adult survivors of childhood and adolescent cancer: retrospective analysis of the Childhood Cancer Survivor Study cohort. *BMJ*. 2009;339:b4606.

15. Mulrooney DA, Armstrong GT, Huang S, Ness KK, Ehrhardt MJ, Joshi VM, Plana JC, Soliman EZ, Green DM, Srivastava D, Santucci A, Krasin MJ, Robison LL, Hudson MM. Cardiac Outcomes in Adult Survivors of Childhood Cancer Exposed to Cardiotoxic Therapy: A Cross-sectional Study. *Ann. Intern. Med*. 2016;164:93–101.

16. van Nimwegen FA, Ntentas G, Darby SC, Schaapveld M, Hauptmann M, Lugtenburg PJ, Janus CPM, Daniels L, van Leeuwen FE, Cutter DJ, Aleman BMP. Risk of heart failure in survivors of Hodgkin lymphoma: effects of cardiac exposure to radiation and anthracyclines. *Blood*. 2017;129:2257–2265.

17. Xavier AC, Costa LJ. Changes in the use of radiation therapy for early classical Hodgkin lymphoma in adolescents and young adults: implications for survival and second malignancies. *Leuk. Lymphoma*. 2015;56:2339–2343.

18. Hoppe RT, Advani RH, Ai WZ, Ambinder RF, Aoun P, Bello CM, Benitez CM, Bernat K, Bierman PJ, Blum KA, Chen R, Dabaja B, Forero A, Gordon LI, Hernandez-Ilizaliturri FJ, Hochberg EP, Huang J, Johnston PB, Kaminski MS, Kenkre VP, Khan N, Maloney DG, Mauch PM, Metzger M, Moore JO, Morgan D, Moskowitz CH, Mulroney C, Poppe M, Rabinovitch R, Seropian S, Smith M, Winter JN, Yahalom J, Burns J, Ogba N, Sundar H. Hodgkin Lymphoma Version 1.2017, NCCN Clinical Practice Guidelines in Oncology. *J. Natl. Compr. Cancer Netw*. 2017;15:608–638.

19. Meyer RM, Gospodarowicz MK, Connors JM, Pearcey RG, Wells WA, Winter JN, Horning SJ, Dar AR, Shustik C, Stewart DA, Crump M, Djurfeldt MS, Chen BE, Shepherd LE. ABVD Alone versus Radiation-Based Therapy in Limited-Stage Hodgkin's Lymphoma. *N. Engl. J. Med*. 2012;366:399–408.

20. Ng A, Brock KK, Sharpe MB, Moseley JL, Craig T, Hodgson DC. Individualized 3D Reconstruction of Normal Tissue Dose for Patients With Long-term Follow-up: A Step Toward Understanding Dose Risk for Late Toxicity. *Int. J. Radiat. Oncol*. 2012;84:e557–e563.

21. van Nimwegen FA, Cutter DJ, Schaapveld M, Rutten A, Kooijman K, Krol ADG, Janus CPM, Darby SC, van Leeuwen FE, Aleman BMP. Simple Method to Estimate Mean Heart Dose From Hodgkin Lymphoma Radiation Therapy According to Simulation X-Rays. *Int. J. Radiat. Oncol*. 2015;92:153–160.

22. Darby SC, Ewertz M, McGale P, Bennet AM, Blom-Goldman U, Brønnum D, Correa C, Cutter D, Gagliardi G, Gigante B, Jensen M-B, Nisbet A, Peto R, Rahimi K, Taylor C, Hall P. Risk of Ischemic Heart Disease in Women after Radiotherapy for Breast Cancer. *N. Engl. J. Med*. 2013;368:987–998.

23. Moignier A, Broggio D, Derreumaux S, Beaudré A, Girinsky T, Paul J-F, Drubay D, Lefkopoulos D, Franck D, Aubert B, Deutsch E, Bourhis J. Coronary stenosis risk analysis following Hodgkin lymphoma radiotherapy: A study based on patient specific artery segments dose calculation. *Radiother. Oncol*. 2015;117:467–472.

24. Bahig H, de Guise J, Vu T, Blais D, Chartrand-Lefebvre C, Nguyen NT, Lavertu S, Guay J-P, Bedwani S, Roberge D. In a Heartbeat: An Assessment of Dynamic Dose Variation to Cardiac Structures Using Dual Source Computed Tomography. *Int. J. Radiat. Oncol*. 2018;102:950–959.

25. Wennstig A-K, Garmo H, Isacsson U, Gagliardi G, Rintelä N, Lagerqvist B, Holmberg L, Blomqvist C, Sund M, Nilsson G. The relationship between radiation doses to coronary arteries and location of coronary stenosis requiring intervention in breast cancer survivors. *Radiat. Oncol*. 2019;14:40.

26. Baker LL, Parker BR, Donaldson SS, Castellino RA. Staging of Hodgkin disease in children: comparison of CT and lymphography with laparotomy. *AJR. Am. J. Roentgenol*. 1990;154:1251–1255.

27. Duane F, Aznar MC, Bartlett F, Cutter DJ, Darby SC, Jagsi R, Lorenzen EL, McArdle O, McGale P, Myerson S, Rahimi K, Vivekanandan S, Warren S, Taylor CW. A cardiac contouring atlas for radiotherapy. *Radiother. Oncol*. 2017;122:416–422.

28. Taparra K, Lester SC, Hunzeker A, Funk RK, Blanchard M, Young P, Herrmann J, Tasson A, Leng S, Martenson JA, Whitaker TJ, Williamson EE, Laack II NN. A Comparison of Proton and X-ray Therapy for Coronary Artery Sparing Using ECG-gated CT with Coronary Angiography for Mediastinal Lymphoma. *Int. J. Radiat. Oncol. • Biol. • Phys*. 2018;102:S87–S88.

29. Lester SC, Taparra K, Hunzeker A, Funk RK, Blanchard M, Young P, Herrmann J, McCollough C, Tasson A, Leng S, Martenson JA, Whitaker TJ, Williamson EE, Laack II NN. Sparing of the Cardiac Valves and Left Ventricle using Proton Therapy with ECG-gated CT with Coronary Angiography for the Treatment of Mediastinal Lymphoma. *Int. J. Radiat. Oncol. • Biol. • Phys*. 2018;102:e277.

30. Allen AM, Pawlicki T, Dong L, Fourkal E, Buyyounouski M, Cengel K, Plastaras J, Bucci MK, Yock TI, Bonilla L, Price R, Harris EE, Konski AA. An evidence based review of proton beam therapy: the report of ASTRO's emerging technology committee. *Radiother. Oncol*. 2012;103:8–11.

31. Mohan R, Grosshans D. Proton therapy – Present and future. *Adv. Drug Deliv. Rev*. 2017;109:26–44.

32. Ntentas G, Dedeckova K, Andrlik M, Aznar MC, George B, Kubeš J, Darby SC, Cutter DJ. Clinical Intensity Modulated Proton Therapy for Hodgkin Lymphoma: Which Patients Benefit the Most? *Pract. Radiat. Oncol*. 2019;9:179–187.

33. Cheson BD, Fisher RI, Barrington SF, Cavalli F, Schwartz LH, Zucca E, Lister TA. Recommendations for Initial Evaluation, Staging, and Response Assessment of Hodgkin and Non-Hodgkin Lymphoma: The Lugano Classification. *J. Clin. Oncol*. 2014;32:3059–3067.

34. Lester SC, Taparra K, Petersen MM, Funk RK, Blanchard MJ, Young PM, Herrmann J, Hunzeker AE, Schultz HL, McCollough C, Tasson AM, Leng S, Martenson JA, Deisher AJ, Whitaker TJ, Williamson EE, Laack NN. Electrocardiogram-Gated Computed Tomography with Coronary Angiography for Cardiac Substructure Delineation and Sparing in Patients with Mediastinal Lymphomas Treated with Radiation Therapy. *Pract. Radiat. Oncol*. 2020;10:104–111.

35. Illidge T, Specht L, Yahalom J, Aleman B, Berthelsen AK, Constine L, Dabaja B, Dharmarajan K, Ng A, Ricardi U, Wirth A, International Lymphoma Radiation Oncology Group. Modern radiation therapy for nodal non-Hodgkin lymphoma-target definition and dose guidelines from the International Lymphoma Radiation Oncology Group. *Int. J. Radiat. Oncol. Biol. Phys*. 2014;89:49–58.

36. Armanious MA, Mohammadi H, Khodor S, Oliver DE, Johnstone PA, Fradley MG. Cardiovascular effects of radiation therapy. *Curr. Probl. Cancer*. 2018;42:433–442.

37. Hahn E, Jiang H, Ng A, Bashir S, Ahmed S, Tsang R, Sun A, Gospodarowicz M, Hodgson D. Late Cardiac Toxicity After Mediastinal Radiation Therapy for Hodgkin Lymphoma: Contributions of Coronary Artery and Whole Heart Dose-Volume Variables to Risk Prediction. *Int. J. Radiat. Oncol. Biol. Phys*. 2017;98:1116–1123.

38. Hoppe BS, Flampouri S, Su Z, Latif N, Dang NH, Lynch J, Joyce M, Sandler E, Li Z, Mendenhall NP. Effective Dose Reduction to Cardiac Structures Using Protons Compared With 3DCRT and IMRT in Mediastinal Hodgkin Lymphoma. *Int. J. Radiat. Oncol*. 2012;84:449–455.

39. Jagsi R, Griffith KA, Moran JM, Ficaro E, Marsh R, Dess RT, Chung E, Liss AL, Hayman JA, Mayo CS, Flaherty K, Corbett J, Pierce L. A Randomized Comparison of Radiation Therapy Techniques in the Management of Node-Positive Breast Cancer: Primary Outcomes Analysis. *Int. J. Radiat. Oncol. Biol. Phys*. 2018;101:1149–1158.

40. Liao Z, Lee JJ, Komaki R, Gomez DR, O'Reilly MS, Fossella F V, Blumenschein GR, Heymach J V, Vaporciyan AA, Swisher SG, Allen PK, Choi NC, DeLaney TF, Hahn SM, Cox JD, Lu CS, Mohan R. Bayesian Adaptive Randomization Trial of Passive Scattering Proton Therapy and Intensity-Modulated Photon Radiotherapy for Locally Advanced Non-Small-Cell Lung Cancer. *J. Clin. Oncol*. 2018;36:1813–1822.